Astron. Astrophys. 156, 261–267 (1986)

ASTRONOMY
AND
ASTROPHYSICS

Ages and metallicities of LMC and SMC red clusters through Hβ and G band photometry★

E. Bica[1] ★★, H. Dottori[2] ★★★, and M. Pastoriza[2]

[1] Observatoire de Meudon, F-92195 Meudon Principal Cedex, France
[2] Universidade Federal do Rio Grande do Sul, Instituto de Fisica, R. Luis Englert s/n°. 90000 Porto Alegre, RS, Brazil

Received June 13, accepted August 2, 1985

Summary. We present narrow band integrated photometry of the Hβ and G band absorption features for 41 LMC and 10 SMC red star clusters. An age-metallicity calibration is provided for the color-color diagram. We derive SWB types between IV and VII for 23 unclassified clusters and discuss their distribution in the age vs metallicity plane. We study the chemical evolution of the Magellanic Clouds (MC): the LMC presents a steeper chemical enrichment slope. An intrinsic metallicity dispersion is found in the LMC chemical evolution, indicating that the gas has been inhomogeneous at any time, prevailing a local enrichment over a global one. One zone models describe the evolution of both Clouds, being the efficiency of star cluster formation larger in the LMC. The LMC presents a burst of star cluster formation at $t = 4.5\,10^9$ yr. We also present new $B-V$ data for fainter SMC clusters, providing an essentially complete color histogram for clusters with globular cluster appearance.

Key words: Magellanic clouds – red star clusters – age-metallicity relationship

1. Introduction

The study of the evolution of star clusters through their integrated light is not simple owing to the difficulty of isolating spectral features sensitive either to age or metallicity. A two dimensional classification scheme for the MC clusters was provided by Searle, Wilkinson and Bagnuolo, 1980 (SWB) based on integrated photometry in the Gunn-Thuan system. Rabin (1982) compared measurements of equivalent widths (W) of Balmer lines and metallic features with synthetic spectra in order to estimate ages and metallicities. Searle (1984) showed that the SWB types IV to VII define a relationship in Rabin's diagram and provided a theoretical age-metallicity grid.

The DDO G band color index $C(42-45)$ is highly correlated with metallicity in the integrated light of old star clusters (McClure and Van den Bergh, 1968: Bica and Pastoriza, 1983: Dottori et al., 1983).

In this paper, we present narrow band photometry, carried out with filters 42 and 45 of the DDO System, as well as a narrow Hβ (FWHM = 27 Å) filter, for red clusters in the MC. This approach presents the advantage of photometric precision over the spectrophotometric equivalent widths, as well as resolution of spectral features with respect to the SWB's photometry.

We present the observations in Sect. 2. We derive an age-metallicity calibration of the reddening corrected $C(42-45)_0$ vs $C(45-H\beta)_0$ diagram and estimate SWB types for clusters not observed previously, as well as discuss the SWB's classification as a function of age and metallicity in Sect. 3. The chemical evolution of each Cloud is discussed in Sect. 4. Supplementary B and V observations for SMC faint clusters and concluding remarks of this paper are given in Sects. 5 and 6 respectively.

2. Observation

Integrated light photometry of 41 LMC and 10 SMC red clusters, as well as of 6 Galactic globular clusters, were carried out in January and November 1984 at the 1 m ESO Cassegrain telescope. The observations were made through the DDO 42 and 45 filters, measuring the G band and continuum respectively (McClure and Van den Bergh, 1968) and through a narrow Hβ (FWHI = 27 Å) interference filter. The integration time in each filter was such as to provide 1% in cluster plus sky count standard deviation, using a 2 s integration base; a sky integration was stopped when the precision level achieved 1% with respect to the cluster plus sky count. This combined precision level led to mean color errors $\epsilon(42-45) = 0.018$ and $\epsilon(45-H\beta) = 0.020$ as well as $\epsilon(m45) = 0.025$, for repeated measurements. For each cluster at least two sky areas at opposite position angles were observed; for clusters in crowded fields, several position angles were sampled. Each night 2 stars were monitored for extinction corrections and a set of 12 standard stars (including DDO's) was observed. For the color $C(45-H\beta)$ we defined the standard values which are listed in Table 1, together with DDO m45 and $C(42-45)$ values. In order to evaluate the errors in the standard system transformation, 15% of the object sample was observed on different nights, resulting in $\epsilon(m45) = \epsilon(42-45) = \epsilon(45-H\beta) = 0.007$. We have listed the results in Table 2: (1) name; (2) diaphragm size in arcsec; (3) m45; (4) $C(42-45)$ and (5) $C(45-H\beta)$.

3. The age-metallicity calibration

The color indexes $C(42-45)$ and $C(45-H\beta)$ have been corrected for reddening using the relations $E(42-45) = 0.23\ E(B-V)$

Send offprint requests to: E. Bica
★ Partly based on observations collected at the European Southern Observatory, La Silla
★★ Fellowship from the Brazilian Institution CNPq
★★★ Humboldt Foundation Fellow

Table 1

Standard Star	m45	C(42–45)	C(45–Hβ)
HD 166	7.425	0.753	0.648
HD 4965	8.079	0.329	0.081
HD 6734	7.876	0.785	0.723
HD 6833	8.150*	1.302*	0.966
HD 8949	7.831	0.937	0.803
HD 13936	7.327	0.282	0.176
HD 21197	9.441	1.264	0.766
HD 48616	8.309	0.557	0.607
HD 51219	8.704	0.705	0.627
HD 52533	8.473	0.275	0.393
HD 224155	7.555	0.288	-0.001
AG 510	11.084	0.422	0.376
AG 513	10.463	0.920	0.800

* Values derived from the present photometry. The DDO original values are 8.476 and 0.912 respectively (Mc Clure, 1976). Variable star ?

and $E(45\text{–H}\beta) = E(45\text{–}48) = 0.31E(B-V)$(McClure, 1979). We adopted $E(B-V) = 0.06$ and $E(B-V) = 0.03$ respectively for the LMC and the SMC (Mould and Aaronson, 1980). For the Galactic globular clusters we used $E(B-V)$ from Bica and Pastoriza (1983). In Fig. 1a we present the reddening corrected diagram $C(42\text{–}45)_0$ vs $C(45\text{–H}\beta)_0$: the Galactic globular clusters show a linear relationship in this diagram. This behaviour is likewise observed for the W of Balmer lines vs W of metallic features (Rabin, 1982) and for the W of metallic features as a function of metallicity (Bica and Alloin, 1985). The globular cluster sequence essentially represents an isochrone for $1.65\,10^{10}$ yr (Vandenberg, 1983; Janes and Demarque, 1983). The MC clusters define a sequence similar to SWB's, as it can be seen in Fig. 1b, where we show the distribution of SWB types in the color-color diagram of the present photometry, for the 27 clusters in common between the two samples. A comparison of Figs. 1a and 1b allows the determination of SWB types for the 23 remaining unclassified clusters. The narrow band photometry provided a larger dynamical range which allowed a sharper separation of SWB types. Particularly, it has been possible to reassign types in some doubtful cases. The SWB types are listed in column 6 of Table 2.

The age-metallicity calibration of the $C(42\text{–}45)_0$ vs $C(45\text{–H}\beta)_0$ diagram consists of a grid which was built according to the following criteria:

a) The metallicity along the Galactic globular cluster isochrone was derived from Bica and Pastoriza, 1983.

(b) In order to constrain the grid at the lower age limit, we have used the blue-red transition object NGC 1868 as well as NGC 2209 (Van den Bergh, 1981; Hodge, 1982).

c) The definition of intermediate isochrones was made through the distribution of SWB types in the plane, together with their age calibration (Hodge, 1983).

d) As a constraint for the metal rich locus at $t \simeq 10^9$ yr, we have used spectrophotometric observations of the Galactic disk clusters NGC 2158 and NGC 2660 (Bica and Alloin, 1985). We have derived two equations, respectively for Hβ and G band, relating the spectrophotometric W and the reddening corrected color indexes, using the 11 clusters in common in both samples.

e) Finally, we took into account the distribution of clusters having age or metallicity determination through individual stars (Hodge, 1983; Mould and Aaronson, 1982; Cowley and Hartwick, 1982, Cohen, 1982).

The resulting grid is shown in Fig. 1. We derive new and homogeneous age and metallicity estimates for the whole cluster sample (Table 2).

The loci of SWB types VI and VII (Fig. 1b) with respect to the grid indicate that the type VI clusters are some billion yr younger than the Galactic globulars and present *only* intermediate metallicities. On the contrary, type VII clusters are, in general, indistinguishable from metal poor Galactic globular clusters. It is also possible that some type VII clusters present younger ages than Galactic Globulars. Thus they should be the metal poor counterparts of type VI. Two examples are NGC 2210 and 1466, which present partially blue horizontal branches (HB),

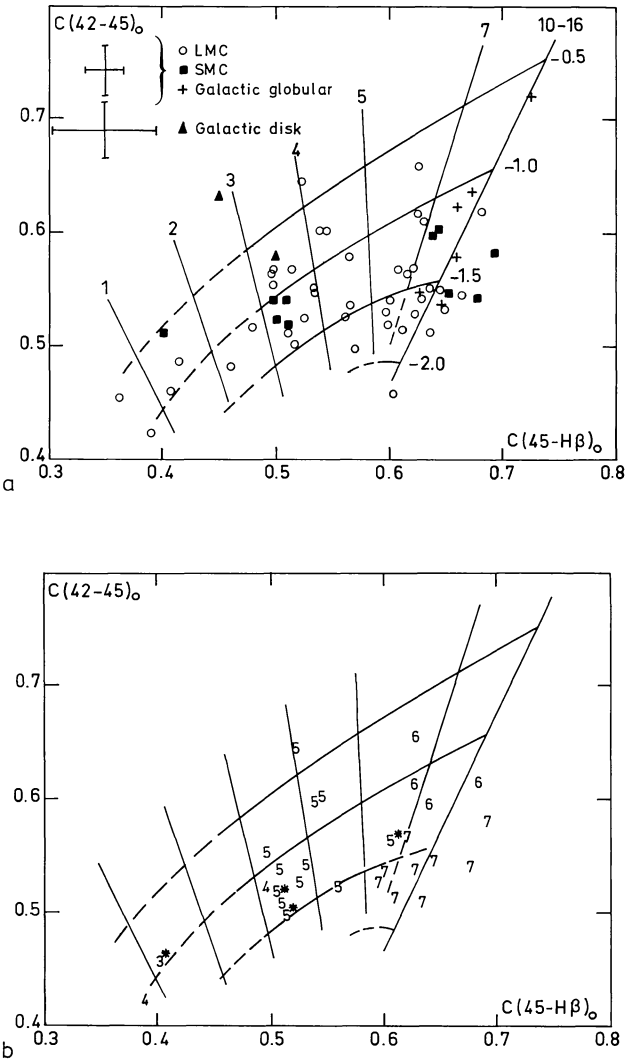

Fig. 1. a The cluster distribution in the reddening corrected color-color plane. Numbers along vertical and horizontal lines are respectively ages in units 10^9 yr and metallicities. **b** Numbers are SWB types. An asterisk denotes transition types as given by SWB (e.g. 5* means type V–VI). The grid is according to **a**.

Table 2

Object	Diaph(")	m_{45}	C(42-45)	C(45-Hβ)	SWB	Age (10^9 yrs)	(Z/Z_0)
SMC							
K3	61	13.580	.553	.662	VII*	⩾10	-1.5 ±0.2
K5	61	14.737	.546	.507	V*	3.2±0.3	-1.1 ±0.2
NGC 121	61	12.788	.590	.701	VII	⩾10	-1.3 ±0.2
NGC 152	61	14.450	.530	.510	IV;V*	3.2±0.3	-1.25±0.25
NGC 339	61	14.350	.549	.686	VII	⩾10	-1.5 ±0.2
NGC 361**	61	13.954	.609	.651	VI*	8±1.5	-1.25±0.2
NGC 411	61	13.616	.525	.520	V-VI,V*	3.4±0.3	-1.3 ±0.2
NGC 416	61	12.863	.605	.648	VI	8±1.5	-1.25±0.2
NGC 419	61	11.993	.545	.518	V	3.5±0.3	-1.2 ±0.2
NGC 643	61	14.538	.519	.410	IV*	1.5±0.3	-0.6 ±0.25
LMC							
NGC 1466	43	13.252	.553	.621	VII	6^{+2}_{-1}	-1.6 ±0.2
NGC 1644	43	14.371	.524	.530	V	3.4±0.4	-1.4 ±0.2
NGC 1651	61	14.079	.580	.532	V*	3.7±0.3	-0.9 ±0.3
NGC 1652	43	14.813	.622	.649	VI*	7^{+2}_{-1}	-1.2 ±0.2
NGC 1718	61	13.739	.577	.634	VII*	7^{+2}_{-1}	-1.4 ±0.2
NGC 1751	61	13.612	.658	.541	V	4±0.3	-0.4 ±0.2
NGC 1754	43	13.373	.546	.663	VII*	⩾10	-1.6 ±0.2
NGC 1777	31	14.454	.500	.434	IV*	1.5±0.25	-0.8 ±0.3
NGC 1783	61	12.324	.567	.517	V	3.3±0.3	-0.9 ±0.4
NGC 1786**	43	12.268	.563	.654	VII*	⩾10	-1.5 ±0.2
NGC 1795	61	14.168	.578	.516	V*	3.3±0.3	-0.9 ±0.4
NGC 1806	61	12.699	.615	.561	V	4.3±0.3	-0.7 ±0.35
NGC 1835	43	11.785	.563	.647	VII	⩾10	-1.6 ±0.2
NGC 1841	61	14.027	.562	.662	VII	⩾10	-1.6 ±0.2
NGC 1846	61	12.813	.615	.561	V	4.3±0.3	-0.7 ±0.35
NGC 1852	61	13.494	.561	.553	V*	4.0±0.3	-1.2 ±0.2
NGC 1868	61	12.809	.469	.380	IV*	0.5	-0.6 ±0.35
NGC 1898	43	13.240	.558	.683	VII*	⩾10	-1.6 ±0.2
NGC 1916	43	11.994	.553	.617	VII*	7^{+3}_{-2}	-1.75±0.2
SL 363	43	13.570	.550	.584	V*	4.6±0.4	-1.4 ±0.3
NGC 1917	61	13.569	.530	.498	IV*-V*	2.8±0.4	-1.1 ±0.2
NGC 1978	61	12.180	.625	.644	VI	$6.6^{+1.4}_{-0.9}$	-1.1 ±0.2
NGC 1987	61	13.387	.438	.408	IV	0.8±0.3	-1.0 ±0.3
SL 506	61	14.932	.538	.545	V*	3.8±0.4	-1.35±0.3
NGC 2005	43	12.685	.543	.642	VII*	>9	-1.7 ±0.2
NGC 2019	43	12.489	.582	.639	VII	7±2	-1.4 ±0.2
IC 2146	61	14.615	.472	.620	VII*	⩾10	<-2.0
NGC 2108	61	13.605	.495	.479	IV*-V*	2.2±0.3	-1.2 ±0.2
NGC 2121	61	13.804	.672	.644	VI	6±0.5	-0.75±0.25
NGC 2154	61	13.552	.539	.580	V	4.5±0.5	-1.5 ±0.25
NGC 2155	61	14.102	.631	.700	VI	⩾10	-1.2 ±0.2
NGC 2162	61	14.091	.541	.546	V	3.8±0.4	-1.35±0.3
NGC 2173	61	13.818	.581	.626	V-VI;VI*	6.5±0.7	-1.4 ±0.2
NGC 2193	61	14.641	.512	.589	V*	4.6±0.5	-1.8 ±0.2
NGC 2203	61	13.511	.592	.584	V	4.7±0.3	-1.1 ±0.2
NGC 2209	61	14.462	.474	.426	III-IV;IV*	1.2±0.3	-0.9 ±0.3
NGC 2210	43	12.557	.543	.616	VII	6^{+3}_{-1}	-1.7 ±0.2
NGC 2213	61	13.863	.515	.536	V-VI;V*	3.5±0.4	-1.5 ±0.25
SL 868	61	12.557	.527	.655	VII	⩾10	-1.75±0.2
NGC 2231	61	14.306	.562	.553	V	4.0±0.3	-1.2 ±0.2
NGC 2257	61	14.033	.528	.630	VII	⩾10	-1.6 ±0.2
GGC							
NGC 104	61	7.860	.736	.749			
NGC 362	61	9.129	.648	.691			
NGC 1261	61	10.993	.621	.659			
NGC 1851	61	9.459	.598	.687			
NGC 1904	61	10.375	.546	.627			
NGC 7078	61	9.211	.554	.671			

* SWB types derived from the present photometry
** Magnitude and color corrected of foreground star

as well as RR Lyrae stars (Hodge, 1984). This suggests that, for metal poor clusters, RR Lyrae and blue HB stars may arise at younger ages than in classical globulars.

Along with NGC 1466 and 2210, the type VII clusters NGC 121, 1786, 1835, 1841 and 2257 contain RR Lyra stars, but none has been detected in the surveys of NGC 339, 2019 and SL 868 (Graham and Nemec, 1984). As well, no RR lyrae have been found in type VI (e.g. NGC 416, 1978 and 2155). Our results indicate that the LMC clusters NGC 1718, 1754, 1898, 1916, 2005 and IC 2146, as well as K3 in the SMC, are worth being surveyed for RR Lyrae.

4. The chemical evolution

We show in Figs. 2a and 2b the chemical evolution of the LMC and SMC respectively. We included in the figures the results for relative oxygen abundances for H II regions (Pagel et al., 1978 and references therein) as well as metal abundances for LMC blue clusters (10^7 < ages < $5\,10^8$ yr), as derived from spectra of individual stars (Cohen, 1982). A definite chemical enrichment occurs in both objects. For the LMC the scatter appears to be intrinsic, therefore suggesting that the gas has been inhomogeneous at any time. This result supports a local rather than global enrichment in the interstellar gas. On the contrary, in the SMC, there is a more homogeneous chemical enrichment. A scatter in the LMC metallicities is also visible in the LMC H II regions + blue clusters set. On the other hand the homogeneity of the chemical enrichment for the SMC older clusters is also present in the SMC H II region data set. We emphasize that although the SMC star cluster sample amounts to 25% of that of the LMC, it is about complete for populous clusters.

Linear regressions yield for the chemical enrichment of the Clouds (t in 10^9 yr units):

$$[Z/Z_\odot] = -0.123t - 0.52$$
$$[Z/Z_\odot] = -0.060t - 0.85$$

for the LMC and SMC respectively.

A steeper slope is found for the LMC, but it is rather ill-defined within the intrinsic dispersion.

The mean metal content for $t \geq 10^{10}$ yr is essentially the same within the error bars and intrinsic metallicity scatter. However, it is striking that the lowest metallicity in the SMC is $[Z/Z_\odot] = -1.5$.

The frequency distribution of ages for the LMC and SMC clusters are shown in Fig. 3. The LMC histogram presents two well-defined maxima, the one at $4.5\,10^9$ yr corresponding to a burst of star formation. The peak in the distribution tail results from the impossibility of separating ages for $t > 10^{10}$ yr. The redistribution of this accumulated peak, following the general trend of the histogram, suggests a primordial cluster formation in the LMC at $t \leq 14 \pm 2\,10^9$ yr. This cumulative effect in the tail of the distribution is also visible in the SMC histogram.

We show the metallicity histograms for the LMC and SMC in Fig. 4. Although the LMC metallicity spread at a given time cannot be described by a simple chemical evolution model which

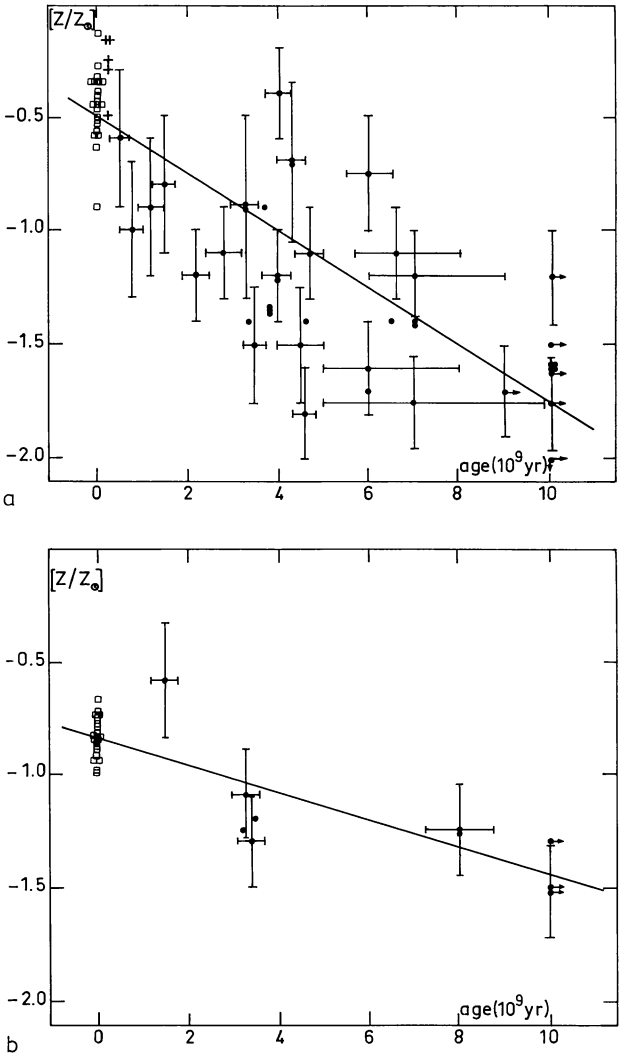

Fig. 2a and b The chemical evolution of the LMC and SMC respectively. For clarity some error bars were omitted. Squares are HII regions and crosses are blue star clusters

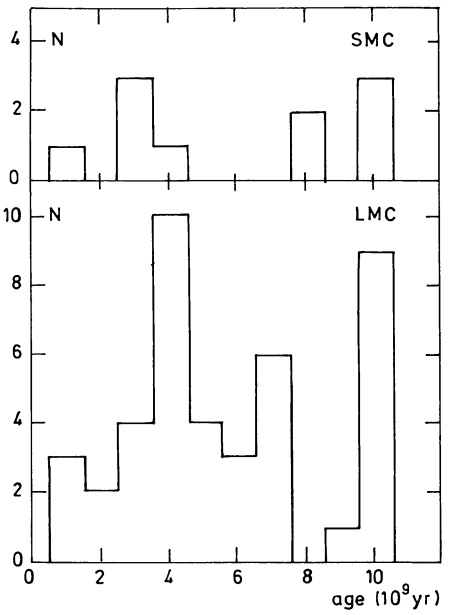

Fig. 3 Age histograms

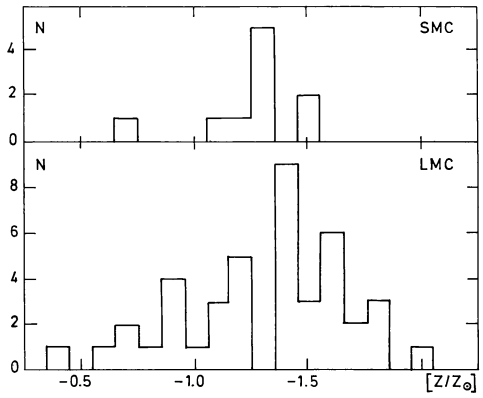

Fig. 4. Metallicity histograms

assumes a homogeneous metal content for the gas as a function of time, we have compared the LMC metallicity histogram with one-zone models (Hartwick, 1976). This is justified by considering that the gas local advances or delays with respect to the mean metal enrichment are implicitly taken into account in the Z histogram. As can be seen in Fig. 5, a model with $C = 10$ (the ratio of the mass ejection rate from star forming regions to the star formation rate) describes the star cluster formation in the LMC. This value confirms the result derived from a smaller sample in a previous paper (Dottori et al., 1983) and it is a factor 5 smaller than that derived for the LMC, from a sample of clusters with classical globular properties (Hartwick and Cowley, 1980). It is important to notice that the one-zone model describes quite well the chemical evolution of the LMC, but not that of the Galactic halo including metal rich globulars (Bica and Pastoriza, 1983). We also compare in Fig. 5 the SMC data with the one-zone

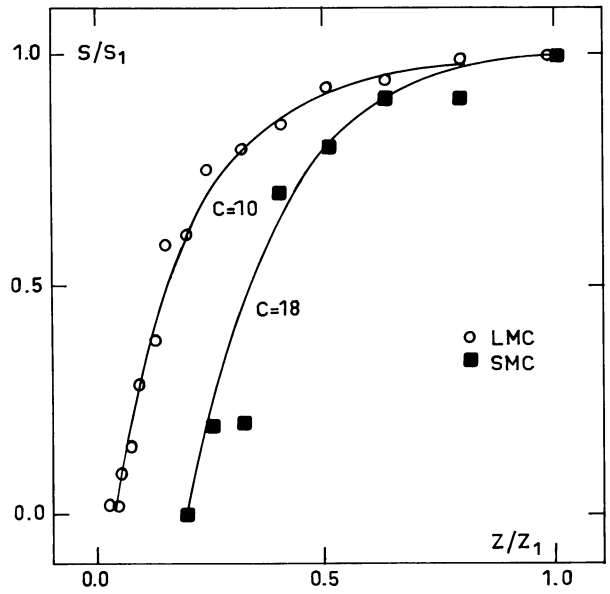

Fig. 5. S is the cumulative number of stars born to the metallicity Z. The subscript 1 denotes the present state of each Cloud. Lines are one-zone models with upper and lower $(Z/Z_\odot)$ limits $(-0.3, -2.0)$ and $(-0.9, -1.6)$ for the LMC and SMC respectively. Circles and squares are the cumulated metallicity histograms respectively for the LMC and the SMC

model. The best fit is obtained for $C = 18$. Owing to the scantiness of clusters, the metallicity limits to be used in the model are not well-defined. However different upper limits $(-0.7 \geq (Z/Z_\odot) \geq -0.9)$ and lower limits $(-1.5 \geq [Z/Z_\odot] \geq -2.0)$ do not change much the value of C obtained for the best fit. Thus, the one-zone model also describes the star cluster formation in the SMC. The smaller value of C found for the LMC implies that star formation processes are more efficient in the LMC than in the SMC.

5. The $B - V$ photometry of SMC clusters

In view of studying the chemical evolution of the SMC through a larger sample of old star clusters, we discuss in this section the completeness of the present SMC red star cluster sample. Van den Bergh (1981) compiled and analyzed the UBV integrated photometry of the Magellanic Cloud clusters, being his SMC sample essentially complete to $V \simeq 13$. In this section we extend the photometry to $V \simeq 15$. The observations were carried out in 1982 at the Cassegrain focus of the 1.6 m telescope in Itajuba, Brazil. We observed 2 stars each night at different airmasses for extinction corrections and about 12 standard UBV stars from Landolt (1973) for the system transformation. The sky background was sampled at different position angles around the cluster, particularly for crowded fields. We list in Table 3 the name, diaphragm size, total number of 60 s integrations on the object, number of nights and the V and $B - V$ measurements with their respective errors. The table contains 27 new clusters with respect to Van den Bergh's list. The 13 clusters in common show a good agreement between the two data sets (Fig. 6) with rms = 0.03 for $B - V$ differences. Following Van den Bergh, we have built the integrated magnitude-color diagram: in our observations we excluded clusters associated with emission, so no new points are seen for $(B - V) < 0.1$. Thus our observations cover the plane for ages $> 10^7$ yr and $13 < V < 15$. From the $B - V$ histogram (Fig. 7), the new sample of blue clusters (not associated with emission) amounts to 40% of the previous one, 43% in the case of the new red star clusters sample $(B - V > 0.6)$ and 300% for the blue-red transition objects $(0.4 < (B - V) < 0.6)$. This confirms Van den Bergh's prediction that many intermediate color clusters would fade below his survey limit, as a result of the evolution and subsequent disappearance of the brightest cluster stars. Also the total number of objects in this class is intrinsically smaller than in the blue or red classes. This is obviously due to the fact that the intermediate color interval with respect to the red class corresponds to a rapid phase in the cluster color evolution, not exceeding 10^9 yr. Also unbounded blue clusters will have disintegrated before reaching the intermediate ages.

The present photometry makes essentially complete the $B - V$ color classification of clusters with globular cluster appearance in the SMC. Since the G Band-Hβ photometry for metallicity and age determinations is valid for $(B - V) > 0.4$, we conclude that the SMC clusters used for the chemical evolution study in Sect. 4 is one third complete and that the sample is 50% complete for clusters with $(B - V) > 0.6$.

6. Concluding remarks

a) The photometric system composed of DDO filters 42 and 45 and a narrow Hβ filter, allows the determination of age and metallicity through the integrated light of red clusters.

Table 3

Name	Diaph (")	n	N	V	B-V
*L1	50	9	3	13.39 ± .03	0.74 .08
K5, L7	44	7	2	13.51 ± .09	0.62 .02
*K3, L8	50	9	3	12.23 ± .17	0.72 .01
K6, L9	44	7	2	14.45 ± .08	0.63 .04
*NGC 121, K2, L10	50	8	3	11.44 ± .07	0.79 .01
*K7, L11	44	7	2	14.40 ± .10	0.74 .03
*NGC 152, K10, L15	50	9	3	13.15 ± .10	0.70 .10
K15, L21	44	3	1	14.55 ± .10	0.50 .07
*K21, L27	50	9	3	13.25 ± .23	0.73 .08
L28	44	3	1	13.58 ± .02	0.52 .02
K27, L36	20	7	2	14.00 ± .11	0.71 .10
L41	44	3	1	12.87 ± .02	0.15 .02
L52	20	3	1	14.58 ± .05	0.15 .06
*K37, L58	44	7	2	14.14 ± .07	0.56 .04
*NGC 339, K36, L59	50	9	3	13.01 ± .20	0.71 .04
K43, L64	44	3	1	14.24 ± .04	0.20 .09
L65	50	3	1	13.79 ± .03	0.24 .04
*K44, L68	50	7	2	13.79 ± .15	0.84 .06
K45, L69	44	3	1	14.65 ± .04	0.53 .05
IC1626, K53, L77	50	3	1	13.43 ± .02	0.34 .03
L80	44	3	1	13.66 ± .03	0.26 .04
K55, L81	44	4	1	14.39 ± .15	0.12 .08
*NGC 411, L60, L82	44	9	3	12.47 ± .07	0.66 .02
*NGC 416, L59, L83	44	8	3	11.62 ± .01	0.73 .01
*NGC 419, K58, L85	60	8	3	10.56 ± .08	0.64 .02
K57, L86	44	4	1	14.58 ± .12	0.40 .10
K61	44	3	1	14.18 ± .04	0.25 .03
K63, L88	44	3	1	14.29 ± .04	0.26 .05
L91	44	6	2	14.42 ± .15	0.64 .07
IC1662, L92	44	3	1	14.20 ± .03	0.12 .03
L95	44	3	1	14.70 ± .09	0.17 .09
K68, L98	44	4	1	15.25 ± .10	0.11 .09
L100	44	2	1	14.73 ± .03	0.61 .03
L102	44	6	2	14.63 ± .08	0.40 .03
L108	44	6	2	14.54 ± .05	0.49 .04
L109	44	7	2	14.77 ± .09	0.59 .03
L110	44	7	2	14.33 ± .14	0.77 .05
NGC 643, L111	44	9	3	13.47 ± .14	0.57 .04
*L113	50	9	3	13.73 ± .28	0.75 .02
L116	44	14	3	15.37 ± .17	0.45 .13

* Objects with previous photometry (Van den Bergh, 1981)

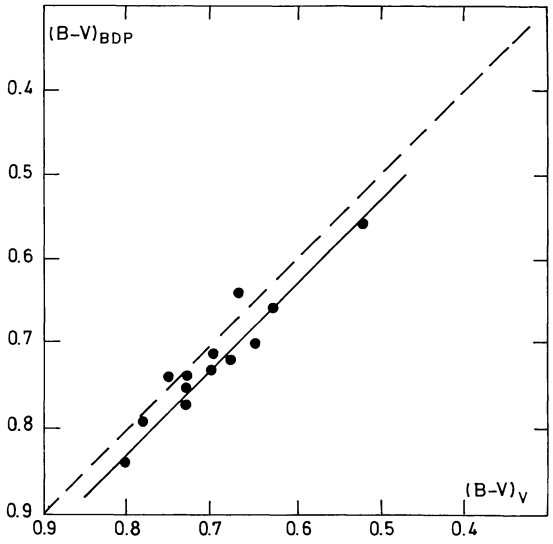

Fig. 6 Comparison of $(B - V)$ between the present photometry and that of Van den Bergh (1981) for the 13 clusters in common between the two data sets

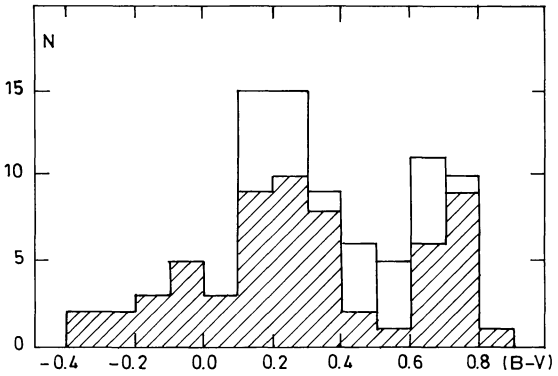

Fig. 7 The $B - V$ histogram: the dark area corresponds to Van den Bergh's (1981) sample; the other part is from the present photometry of clusters with $V \geq 13$

b) We derived an age metallicity calibration corresponding to the color-color diagram.

c) We have estimated SWB types for 23 new cluster. The SWB classification has a larger dynamical range in the present photometry, leading to a better understanding of types VI and VII as a function of age and metallicity.

d) We have obtained ages and metallicities for 41 LMC and 10 SMC red star clusters, which allow direct estimate of the chemical evolution in both Clouds.

e) An intrinsic metallicity scatter is observed along the chemical evolution of the LMC. The LMC presents a steeper chemical enrichment slope.

f) The LMC presents a burst of star cluster formation at $t = 4.5\,10^9$ yr.

g) One-zone models describe quite well the evolution of both Clouds, being the efficiency of star cluster formation in the LMC larger than in the SMC.

h) We present 27 new B and V observations for SMC clusters. These results make essentially complete the $B - V$ color classification of clusters with globular cluster appearance in the SMC.

Acknowledgments: We would like to thank the ESO staff at la Silla as well as Alex Schmidt for assistance during observations and/or reductions. We are indebted to D. Alloin for reading the manuscript and for the interesting suggestions. H. Dottori acknowledges the hospitality at the Astronomisches Institut der Ruhr Universität Bochum.

References

Bica, E., Alloin, D.: 1985, submitted to *Astron. Astrophys.*
Bica, E., Pastoriza, M.: 1983, *Astrophys. Space Sci.* **91**, 99

Cohen, J.G.: 1982, *Astrophys. J.* **258**, 143
Cowley, A.P., Hartwick, F.D.: 1982, *Astrophys. J.* **259**, 89
Dottori, H., Pastoriza, M., Bica, E.: 1983, *Astrophys. Space Sci.* **91**, 79
Graham, J.A., Nemec, J.M.: in Structure and Evolution of the Magellanic Clouds, ed. S. Van den Bergh and K.S. Boer, Dordrecht: Reidel, p. 37
Hartwick, F.D.: 1976, *Astrophys. J.* **209**, 418
Hartwick, F.D., Cowley, A.P.: 1980., in Star Clusters, IAU *Symp* 85, ed. J.E. Hesser, Dordrecht: Reidel. p. 335
Hodge, P.W.: 1982, *Astrophys. J.* **256**, 447
Hodge, P.W.: 1983, *Astrophys. J.* **264**, 470
Hodge, P.W.: 1984, in Structure and Evolution of the Magellanic Clouds. ed. S. Van den Bergh and K.S. Boer, Dordrecht: Reidel, p. 7
Janes, K.A., Demarque, P.: 1983, *Astrophys. J.* **264**, 206
Landolt, A.U.: 1973, *Astron. J.* **78**, 959
McClure, R.D.: 1976, *Astron. J.* **81**, 182
McClure, R.D.: 1979, *Dudley Observatory Report*, No. 14, p. 83
McClure, R.D., Van den Bergh, S.: 1968, *Astron. J.* **73**, 313
Mould, J., Aaronson, M.: 1980, *Astrophys. J.* **240**, 464
Mould, J., Aaronson, M.: 1982, *Astrophys. J.* **263**, 629
Pagel, B., Edmunds, M., Fosbury, R., Webster, B.: 1978, *Monthly Notices Roy. Astron. Soc.* **184**, 569
Rabin, D.: 1982, *Astrophys. J.* **261**, 85
Searle, L.: 1984, in Structure and Evolution of the Magellanic Clouds. ed. S. Van den Bergh and K.S. Boer, Dordrecht: Reidel, p. 13
Searle, L., Wilkinson, A., Bagnuolo, W.G.: 1980, *Astrophys. J.* **239**, 803
Vandenberg, D.A.: 1983, *Astrophys. J. Suppl.* **51**, 29
Van den Bergh, S.: 1981, *Astron. Astrophys. Suppl.* **46**, 79